

Transient Solidlike Behavior near the Cylinder/Disorder Transition in Block Copolymer Solutions

Moon Jeong Park,[†] Kookheon Char,^{*,†} Timothy P. Lodge,^{*,‡} and Jin Kon Kim[§]

School of Chemical and Biological Engineering and NANO Systems Institute, National Core Research Center, Seoul National University, Seoul 151-744, South Korea, Department of Chemical Engineering and Materials Science and Department of Chemistry, University of Minnesota, Minneapolis, Minnesota 55455, and National Creative Research Center for Block Copolymer Self-Assembly, Department of Chemical Engineering and Chemistry, Pohang University of Science and Technology, Kyungbuk 790-784, South Korea

Received: November 3, 2005; In Final Form: March 16, 2006

A nearly symmetric polystyrene-*block*-polyisoprene diblock copolymer dissolved at a concentration of 40% in styrene-selective solvents exhibited a cylinder-to-disorder transition upon heating. The solvents used were diethyl phthalate (DEP) and 75:25 and 50:50 mixtures of DEP with di-*n*-butyl phthalate (DBP). In DEP, the most styrene-selective of the three solvents, rheological measurements indicated a distinct plateau in the temperature-dependent elastic modulus across the 8 °C interval above the order–disorder transition temperature, $T_{\text{ODT}} = 116$ °C. Previous small-angle neutron scattering measurements in this regime indicated the equilibrium phase to be a liquidlike solution of approximately spherical micelles. An isothermal frequency sweep in this regime indicated a very long relaxation time. Annealing eventually led to the recovery of liquidlike rheological response, over a time scale of hours. Qualitatively similar phenomena were also observed in 75:25 DEP/DBP and 50:50 DEP/DBP solutions, except the fact that the temperature window of the transient response is narrow and the time scale for the recovery diminishes significantly. Neither small-angle X-ray scattering nor static birefringence gave any clear signature of the transient structure. The structure that leads to the transient rheological response is attributed to micellar congestion due to the slow relaxation of anisotropic micelles into an equilibrium distribution of micelles. Possible origins of the remarkable solvent selectivity dependence are also discussed.

Introduction

In recent years a great deal of attention has been devoted to the order–disorder transition (ODT) in block copolymer melts and solutions.^{1–4} One particularly interesting aspect of the ODT emerging from the experimental results is that the disordered state may be directly accessed from lamellae,^{5–7} hexagonal cylinders (HEX),^{8,9} gyroid (G),^{10,11} or body-centered cubic (BCC) spheres,^{12,13} even though Leibler's mean-field theory¹ anticipates the first-order phase transition between a disordered state and a BCC lattice of spherical micelles for any composition except for perfect symmetry. Fredrickson and Helfand demonstrated that substantial spatial fluctuations in composition could stabilize the disordered phase³ and therefore accounted for the direct access to various ordered states. Extensive experimental evidence of such fluctuations has been obtained,^{10,14–17} and a variety of other theoretical approaches have been documented.^{13,16–25} Nevertheless a quantitative theory of the ODT is not yet available, and experiments continue to reveal new complexities.

For asymmetric block copolymers, which adopt the BCC phase below the ODT, extensive effort has defined the pathway from the ordered lattice to the disordered state; strong evidence has been presented of spherical micelles in a liquidlike,

disordered state just above the ODT.^{13,25–31} In the case of the HEX/disorder transition, however, relatively few reports have addressed the same regime.^{8,9,32–34} We have recently shown by small-angle neutron scattering (SANS) on “core-labeled” styrene–isoprene (SI) diblocks in selective solvents that there is a significant range of temperature over which micelles persist above T_{ODT} , for both BCC/disorder and HEX/disorder transitions. Specifically, through the use of symmetric PS-deuterated PI (PS-*d*PI) and deuterated PS–PI (*d*PS–PI) diblock copolymers in selective solvents³³ and contrast matching of the scattering length density between the solvent and the corona blocks, the micellar form factor is simplified significantly. Both a model-independent generalized indirect Fourier transformation and direct model fitting with a spherical form factor combined with the Percus–Yevick structure factor³⁵ indicated the existence of ca. 50 vol % hard spheres just above the ODT. Most micelles were also found to dissociate into free chains around a critical micelle temperature (CMT), which is experimentally located by a distinct decrease in the size, aggregation number, and volume fraction of micelles. Notably, regardless of the different ordered microstructures prior to the disordered state, i.e., BCC and HEX, the CMT is approximately 20–30 °C higher than the T_{ODT} . Two transitions, one first-order thermodynamic transition between the ordered phase and disordered micelles (ODT) and the other a crossover between disordered micelles and fully disordered (CMT), were identified. As a result, three distinct regimes were defined: *ordered state*–ODT–*disordered micelles*–CMT–*mean-field regime*.

* Authors to whom correspondence should be addressed. E-mail: khchar@plaza.snu.ac.kr; lodge@chem.umn.edu.

[†] Seoul National University.

[‡] University of Minnesota.

[§] Pohang University of Science and Technology.

A recent paper by Balsara and co-workers³⁴ reports similar phenomena for the HEX/disorder ODT in an SI diblock melt. An important conclusion from their work, and indeed from many of previous reports, is that different experimental probes of the ODT (e.g., rheology, SANS, small-angle X-ray scattering (SAXS), electron microscopy, and static birefringence) can exhibit different sensitivities to subtle features of the structure. In the present study, we reexamine the vicinity of the ODT in concentrated block copolymer solutions undergoing the HEX/disorder transition, by combining rheology, SAXS, and static birefringence. The block copolymer concentration, composition, and molecular weight are very similar to those used in our recent SANS study.³³ However, in this case, we also varied the solvent quality by mixing two different solvents. The principal new result is the emergence of a long-lived transient state in the rheological properties of the solutions just above the ODT that disappears over a time scale that depends strongly on solvent selectivity. No obvious signature of this transient state is apparent in both SAXS and static birefringence.

Experimental Section

Materials. The polystyrene-*block*-polyisoprene diblock copolymer used in the present study was synthesized by a standard anionic polymerization procedure.³⁶ The block molecular weights, $M_{PS} = 15\,400$ g/mol and $M_{PI} = 14\,400$ g/mol, were determined by a combination of size-exclusion chromatography and ¹H NMR, and the sample is designated as SI(15–14). The polydispersity index by size-exclusion chromatography is 1.02. Two PS-selective solvents, diethyl phthalate (DEP) and di-*n*-butyl phthalate (DBP), were obtained from Aldrich. Solutions of SI(15–14) in pure DEP, in a mixture of 75:25 vol % DEP/DBP and in a mixture of 50:50 vol % DEP/DBP were prepared at a block copolymer concentration of 40 vol %. The 40% block copolymer solutions were specifically selected to have an access to the HEX/disorder transition as a function of temperature.^{33,36,37}

Rheology. An Advanced Rheometrics Expansion System (ARES) was used to measure the dynamic storage modulus (G') and loss modulus (G'') of SI(15–14) solutions with a parallel plate fixture (40 mm diameter and ca. 0.5–1 mm gap). All of the measurements from 30 to 130 °C were performed in the linear viscoelastic regime with a small strain amplitude of 0.01. The temperature control was accurate within ± 0.5 °C, and all of the measurements were taken under nitrogen atmosphere. Temperature scans were carried out at a heating rate of 0.5 °C/min and at a fixed low frequency of 0.5 rad/s; frequency sweeps were also performed at selected temperatures.

Static Birefringence. Static birefringence measurements were performed on a home-built apparatus.³⁸ Vertically polarized light from a He–Ne laser was directed through the sample and a horizontally polarized analyzer placed before a photodiode detector. Samples in disordered states or in an ordered state with isotropic domains do not depolarize the light, and thus no signal is recorded, whereas a well-developed hexagonal cylinder phase is birefringent. The solution was confined between glass disks sealed with a high-temperature adhesive and subjected to a slow temperature increase (less than 0.5 °C/min). Phase transitions are indicated by the abrupt appearance or disappearance of transmitted intensity.

Small-Angle X-ray Scattering. Synchrotron SAXS measurements were carried out at the 4C2 SAXS beam line at the Pohang Light Source (PLS) using a beam with $\lambda = 1.54$ Å ($\Delta\lambda/\lambda = 5 \times 10^{-4}$) and a two-dimensional position-sensitive detector with 2048×2048 pixels. The sample-to-detector distance was fixed at 2.16 m. Solutions were sealed under inert atmosphere

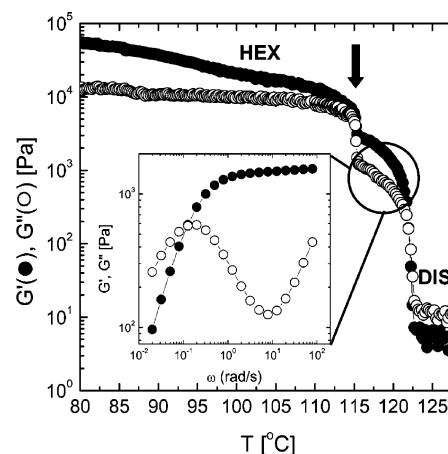


Figure 1. Representative dynamic moduli, G' and G'' , as a function of temperature for the 40% SI(15–14) in DEP. Inset shows a plot of $\log G'$ and $\log G''$ against $\log \omega$ for the same solution at 117 °C at which the solution shows the solidlike behavior in the frequency range $\omega > 0.12$ rad/s. The thick black arrow denotes the HEX/DIS (disordered micelles) transition.

in 1.5 mm quartz capillaries (Charles Supper Co.), and the capillaries were then placed in the sample holder. Sample temperatures were controlled to within ± 0.2 °C using a thermostated brass block. The resulting two-dimensional scattering images were circularly averaged to obtain the traces of intensity plotted against scattering wave vector q ($q = 4\pi \sin(\theta/2)/\lambda$, where θ is the scattering angle).

Results

Figure 1 shows the variation of G' and G'' for 40% SI(15–14) in DEP as a function of temperature. Typically, the ODT is identified by a precipitous drop in both G' and G'' upon heating. In the present study, however, G' shows a distinct drop at around 116 °C but then shows a distinct shoulder before dropping again near 123 °C. The first change in G' , indicated by a thick black arrow, is the equilibrium ODT from the HEX phase to disordered micelles (DIS), as documented elsewhere.³³ The origin of the subsequent plateau is not immediately apparent. One notable feature is a solidlike frequency response in G' immediately above the ODT in frequency range $\omega > 0.12$ rad/s, as shown in the inset of Figure 1, which shows a log–log plot of G' and G'' against frequency ω at 117 °C. Note here that in the frequency range $\omega < 0.12$ rad/s it shows more liquidlike behavior, but $G' \approx \omega^1$ and $G'' \approx \omega^{0.5}$, implying that it is not fully in the terminal regime. The second plateau is reproducible, in the sense that when the sample is fully disordered at higher temperature, then annealed below the ODT and reheated, the plateau returns. We have also taken care to establish that there is no significant sample degradation or solvent evaporation.

In the previous SANS measurements there was no evidence of an ordered structure above the ODT, in contrast to the rheological signature shown in Figure 1. As SANS profiles tend to be relatively broad and might therefore obscure subtle features, we performed synchrotron SAXS experiments on this solution to look for any evidence for the ordered structure over this temperature range. Figure 2 shows the SAXS profiles (scattering intensity $I(q)$ vs scattering vector q) for the 40% SI(15–14) in DEP measured at different temperatures. Measurements were made with a heating rate of 1 °C/min, and an additional 3 min of equilibration time was allowed for every 1 °C increase. Below 115 °C, the higher-order peak at $\sqrt{3}q_{\max}$,

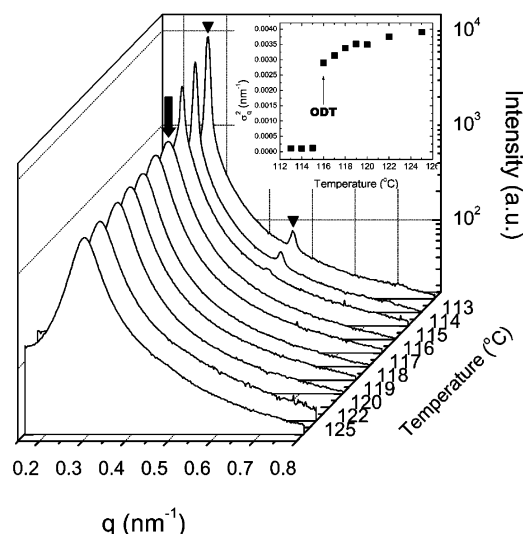


Figure 2. SAXS profiles for the 40% SI(15-14) in DEP as a function of temperature. The black inverted triangles in the SAXS profile measured at 113 °C indicate the Bragg reflections corresponding to the HEX phase. T_{ODT} is located at 116 °C as shown by a thick black arrow. The discontinuous change in the full width at half-maximum near the ODT is also evident in the inset.

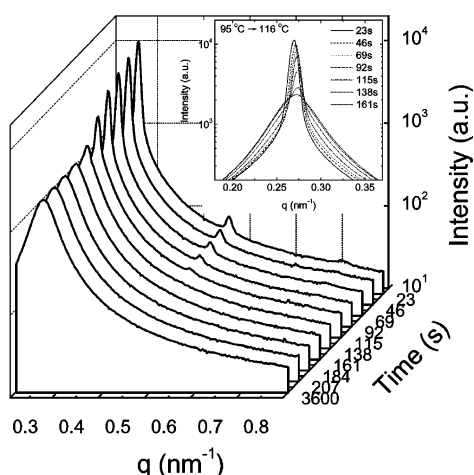


Figure 3. Time evolution of scattering intensity for the 40% SI(15-14) in DEP after a temperature jump from 95 to 116 °C. The change of the first peak intensity as a function of annealing time is also shown in the inset.

as indicated by an inverted black triangle, represents the microphase-separated HEX structure, which completely disappears at a temperature between 115 and 116 °C. Furthermore, the full width at half-maximum (σ_q) of the first-order peak increases abruptly at 116 °C, signaling the ODT for this solution, as shown in the inset of Figure 2. Consequently, T_{ODT} is located between 115 and 116 °C, which is in excellent agreement with the rheological data shown in Figure 1. Just above T_{ODT} , we are unable to find any sign of an ordered structure. The main peak intensity originating from the intermicellar interaction becomes weaker upon further heating, indicating the disordered micellar solution, consistent with the SANS experiments.

We also tried to monitor the HEX/DIS transition in real time by measuring the time-dependent SAXS profiles after a temperature jump from 95 to 116 °C. Since the exposure time for the synchrotron SAXS measurements was 23 s, it is thus possible to monitor structural changes every 23 s. It is interesting to note in Figure 3 that the entire dissolution of the ordered HEX phase occurs between 115 and 138 s and there is no metastable ordered

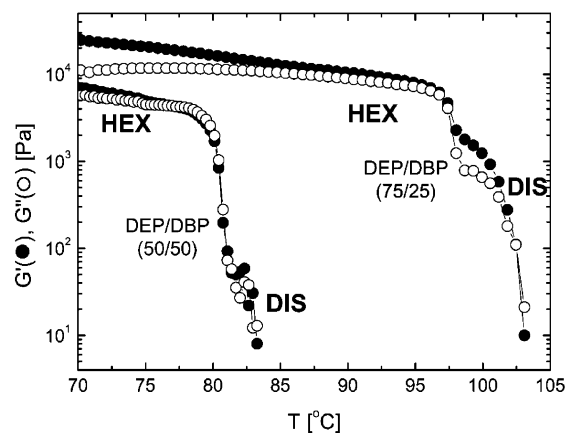


Figure 4. Representative G' and G'' as a function of temperature for the 40% SI(15-14) in DEP/DBP (75:25 vol %) mixture and the 40% SI(15-14) in DEP/DBP (50:50 vol %) mixture. Both solutions represent the ODTs at around 97 and 80 °C, respectively.

structure such as BCC, indicating that the solidlike behavior does not originate from an ordered structure with long-range order. We can also conclude that the intermediate rheological plateau is not associated with a broad coexistence region between HEX and DIS.

Returning to the two-step transition in the shear moduli in the vicinity of the ODT, it clearly is of interest to ascertain whether the same phenomenon is observed in related solutions. One way to do this is to modulate the solvent selectivity at a fixed copolymer concentration, whereby the primary effect is to vary the value of T_{ODT} . In the case of dialkyl phthalate diluents, the solvent selectivity for the PS block can be easily tuned by changing the length of the alkyl group. For example, dioctyl phthalate (DOP) is neutral for both PS and PI blocks, DBP is slightly selective for PS blocks, DEP is more selective, and dimethyl phthalate (DMP) is strongly PS-selective. In this work we chose DEP ($T_{\text{ODT}} \approx 115$ °C) and DBP ($T_{\text{ODT}} \approx 40$ °C) as PS-selective solvents since they allow us to have access to the optimized temperature range to rule out any artifacts caused by solvent evaporation. The examined solvent systems are: DEP, DEP/DBP (75:25 vol %), and DEP/DBP (50:50 vol %) mixtures.

The changes of G' and G'' as a function of temperature for 40% SI(15-14) in DEP/DBP (75:25) and in DEP/DBP (50:50) are represented in Figure 4. For the DEP/DBP (75:25) solution, the HEX/DIS transition is located at 97 °C, and a second sharp decrease in G' and G'' is observed near 102 °C. The temperature range for the two-step transition is thus 5 °C, which is narrower than the 8 °C temperature interval for the solution in pure DEP. The DEP/DBP (50:50) solution, which shows the least selectivity toward the PS block, gives a barely perceptible indication of the two-step transition. These data confirm the two-step transitions for the HEX/DIS transitions, but the temperature window between the two transitions is quite sensitive to the solvent selectivity (or, conceivably, to the absolute temperature). It is perhaps worth noting at this point that as the phenomenon diminishes at lower temperatures and as the solvents are less PS-selective, the glass transition of PS is not playing any role.

To investigate the temporal stability of the solidlike rheological response, the time evolution of G' and G'' was measured at a fixed temperature just above the ODT. As shown in Figure 5 for the SI(15-14) in DEP/DBP (75:25), G' and G'' show a clear crossover (i.e., from $G' > G''$ to $G' < G''$) after about 1000 s of isothermal annealing, and both moduli decrease

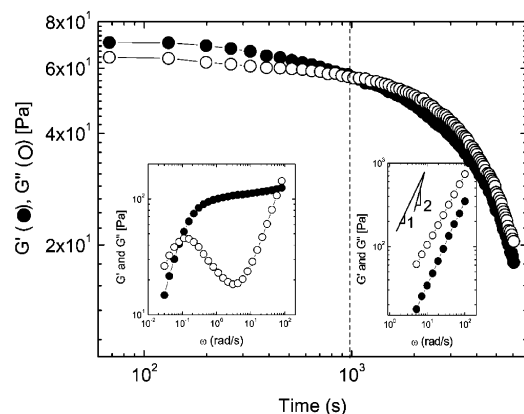


Figure 5. Time evolution of G' and G'' for the 40% SI(15-14) in DEP/DBP (75:25 vol %) mixture annealed at 97 °C, clearly showing the crossover behavior at around 1000 s. The log-log plots of G' and G'' against ω before and after the crossover time are also shown in the inset. After 1000 s of annealing, all of the G' and G'' data are close to $G' \approx \omega^2$ and $G'' \approx \omega^1$, indicating the terminal behavior.

substantially. The log-log plots of G' and G'' against frequency ω before and after the crossover time are shown in the inset, indicating distinctly different frequency-dependent behaviors. Prior to 1000 s of annealing the solution shows the solidlike behavior, whereas the response is close to terminal behavior (i.e., $G' \approx \omega^2$ and $G'' \approx \omega^1$) after annealing more than 1000 s. For fully disordered micellar solutions, the data in the low-frequency regime are difficult to obtain due to the limited torque range of the rheometer. However, the main conclusion from this experiment is that the plateau in the moduli reflects a long-lived but transient state.

The induction time for the crossover from a solidlike to a liquidlike state is also correlated with the solvent selectivity. For SI(15-14) in DEP, it takes a few hours to reach the crossover point between G' and G'' , whereas the crossover occurs within a few seconds when annealing the solution in DEP/DBP (50:50), which is actually on the edge of the detection limit. This observation indicates that the phenomenon does not originate from the solution viscosity. The viscosity of pure DEP at 20 °C is 12 mPa s while that of DBP at the same temperature is 21 mPa s. Therefore the viscosities are ranked in the order of DEP/DBP (50:50) > DEP/DBP (75:25) > DEP.

Given the kinetic nature of the plateau, it is natural to consider whether the two-step transition observed during the heating scan is thermoreversible; i.e., do these solutions follow the same phase sequence progression during both heating and cooling scans? Figure 6a shows the G' traces for 40% block copolymer solutions during heating (filled circles and squares) and cooling (open circles) scans. The initial heating scan, followed by the cooling scan, was performed at a constant rate of ± 0.5 °C/min. For 40% SI(15-14) in DEP it is apparent that G' only increases abruptly at around 116 °C during the cooling scan, signaling the direct DIS to HEX transition exactly at the same ODT as the heating scan. The absence of the two-step transition for the cooling scan indicates that the solidlike feature is a metastable state accessed only upon melting. In other words, the disordered micelles are able to transform directly into hexagonal cylinders without going through the transient solidlike state. The hysteresis behavior for the 40% SI(15-14) in DEP/DBP (75:25) is similar to the behavior of the 40% (15-14) in DEP, and we also note that G'' traces during heating and cooling scans show similar hysteresis behavior (data not shown).

In Figure 6b, the temperature dependence of static birefringence is presented for the 40% SI(15-14) solution in DEP.

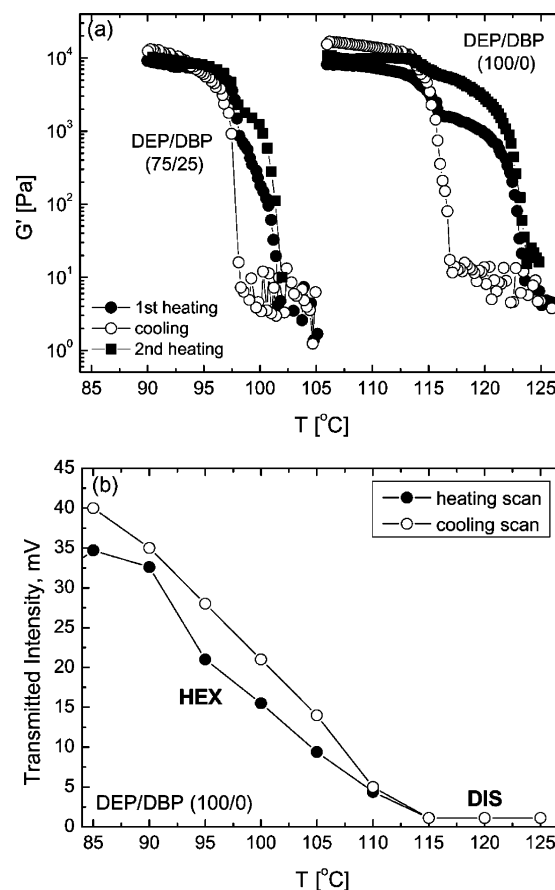


Figure 6. (a) Traces of G' during heating (filled symbols) and cooling (open circles) scans for the 40% SI(15-14) in DEP and the 40% SI(15-14) in DEP/DBP (75:25 vol %) showing distinct hysteresis at the vicinity of the ODT. (b) Static birefringence of the 40% SI(15-14) in DEP during heating (filled circles) and cooling (open circles) scans indicating the isotropic phase in the temperature range showing the hysteresis just above the ODT.

During the heating scan, the birefringence signal gradually decreases after 85 °C, and the birefringence disappears at around 115 °C. Due to the anisotropy of the ordered cylindrical phase, this “on-off” birefringence behavior as a function of temperature is consistent with the phase sequence cylinders to disordered micelles. Particularly, it implies that the disordered solution is composed of approximately isotropic micelles rather than long cylindrical micelles. Note that the measured birefringence within the HEX cylindrical phase is a complicated function of grain size, degree of segregation, and so forth, which is why the signal increases steadily on further cooling.³⁹ During the cooling scan, the “off-on” birefringence behavior takes place at the same temperature as the heating scan, indicating that the disordered micellar solution directly packs into cylinders at the ODT, which is in excellent agreement with the rheology results shown in Figure 6a. It is perhaps worth noting a distinction between these results and those of Balsara et al.;³⁴ in their case, of an SI diblock copolymer melt, the cylinder phase could not be readily formed upon cooling.

Discussion

The two main questions to be addressed are (i) what is the nature or origin of the transient structure that exhibits a clear signature only in rheology and (ii) why is its lifetime so dependent on solvent selectivity?

It seems reasonable to suppose, given that the equilibrium state just above the ODT is a disordered liquid of spherical

micelles that the transient structure contains either too many micelles and/or some anisotropic micelles that have not fully relaxed. The plateau in G' could well result from micellar congestions, which would not give any scattering or birefringence structure. We are inclined to suspect that these micelles also have some anisotropy; i.e., they are ellipsoidal. This seems intuitively reasonable in that the melting of a lattice of cylindrical micelles could give rise, at least initially, to elongated structures. Such a structure would not necessarily cause appreciable birefringence unless there is coherent orientation on the micron scale. It is also believed that such a structure would not affect the small-angle scattering. For example, in the previous SANS study,³³ a spherical micellar form factor and an ellipsoidal form factor with an average ellipticity of 1.3 could represent the data equally well.

An additional piece of evidence in favor of some micellar anisotropy is the following. We examined the DEP solution in a Rheometrics DMTA rheometer in a laboratory SAXS beam⁴⁰ and oriented the cylinder phase by the application of a large amplitude oscillatory shear. This yielded a clear “two-spot” scattering pattern perpendicular to the flow direction; the two-spot pattern for the 40% SI(15–14) in DEP obtained at 105 °C after applying a shear strain of 50% at a shear frequency of 1 rad/s for 1 h is illustrated in Figure 7a. After being heated to 117 °C and passing through the ODT, with a heating rate of 1 °C/min, the two-spot pattern persists for about 5 min, indicating some residual, microscopic anisotropy. This would not be expected if the cylinders broke up immediately into spherical micelles. Interestingly, the two-spot pattern eventually decays to an isotropic ring, as shown in Figure 7c, but at intermediate times, multiple pairs of spots around the principal (q^*) scattering ring are obtained, as shown in Figure 7b, and also these spots persist for about half an hour. This suggests local reorientation and breakup of an anisotropic structure. It should be pointed out at this point that the shear-alignment experiment allows us to follow the dissolution of the transient structure into disordered spherical micelles for about 30 min, since we noted that the solution began to flow slowly out of the measuring gap. Note that this time is considerably shorter than the few hours of annealing possible with both static SAXS and rheology measurements.

We consider three possible explanations for the solvent dependence. First, the more selective solvent (DEP) corresponds to a lower critical micelle concentration, and therefore a lower number density of isolated chains (“unimers”) above the ODT. In this scenario, the slower relaxation of the transient structure is due to the lower rate of exchange of chains among micelles. This could inhibit the equilibration in both the number density and the mean aggregation number of the micelles. We are not persuaded by this argument, however, for the following reason. As shown in many phase diagrams for SI copolymers in dialkyl phthalates,^{33,41,42} the ODT is close to the dilute solution CMT; i.e., the lattice falls apart near the temperature where the solvent penetrates the micelle cores to a significant degree and the number of free chains increases. Thus the region above the ODT should also correspond to a significant increase in the number of free chains.

A second possibility is that the higher interfacial tension in a more selective solvent inhibits micellar equilibration. One observation is the difference in domain spacing of block copolymer solutions in DEP, DEP/DBP (75:25), and DEP/DBP (50:50) just above the T_{ODT} values. For the DEP solution, $q^* = 0.271 \text{ nm}^{-1}$ at 116 °C, $q^* = 0.281 \text{ nm}^{-1}$ at 97 °C for DEP/DBP (75:25), and $q^* = 0.282 \text{ nm}^{-1}$ at 79 °C for DEP/DBP

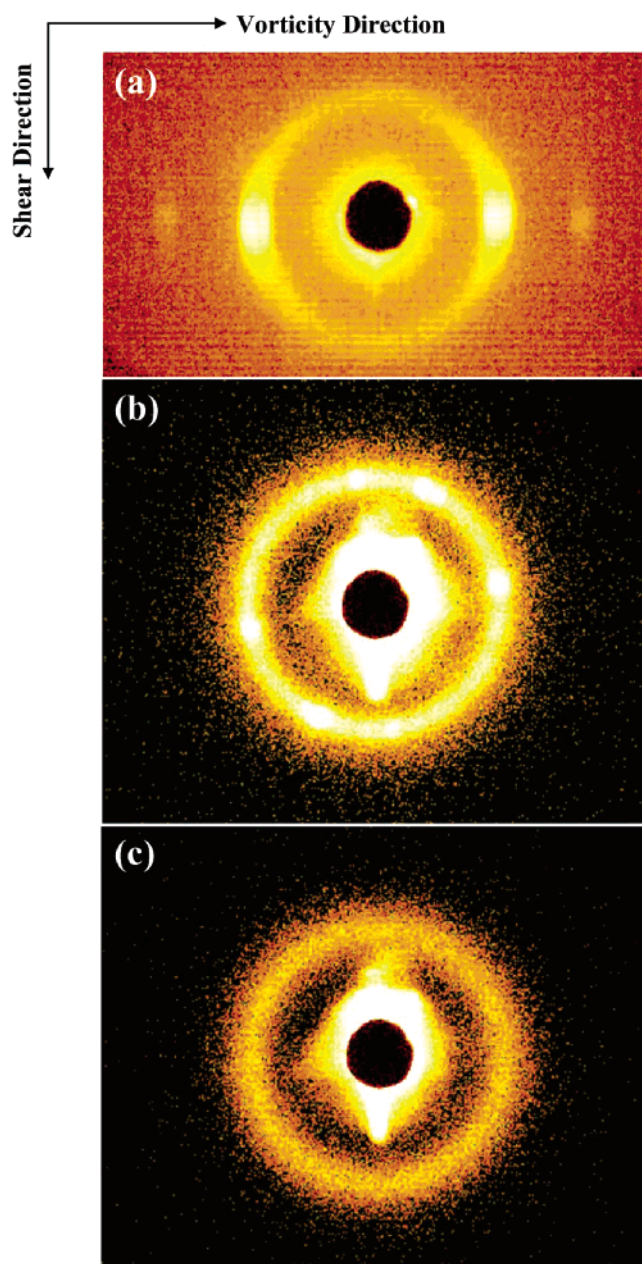


Figure 7. Two-dimensional SAXS patterns obtained from the 40% SI(15–14) in DEP with the X-ray beam directed along the shear gradient direction measured: (a) at 105 °C after applying a shear strain of 50%, (b) at 117 °C after being heated from 105 °C at a heating rate of 1 °C/min without applying shear, and (c) at 117 °C after 30 min of annealing.

(50:50). In other words, the domain spacing of the DEP solution is 23.2 nm, which is larger than 22.3 nm for other DEP/DBP solutions. This suggests stronger chain stretching and therefore a higher interfacial tension. The rapid transition from hexagonal cylinders to congested micelles for PS-*b*-PI in DEP rather than the PS-*b*-PI in (DEP + DBP) mixed solvent could be driven by the higher interfacial tension between the “PI core” and “PS + DEP” than that of “PI core” and “PS + DBP”.⁴³ However, after the formation of congested micelles, the final equilibration of congested micelles could be inhibited by the same interfacial tension and be quite dependent on the aggregation number and the anisotropy of micelles.

A third, possibly more intriguing, explanation emerges from the recent experiments of Balsara et al.³⁴ and the theoretical treatment of Wang et al.¹⁹ They have suggested that the

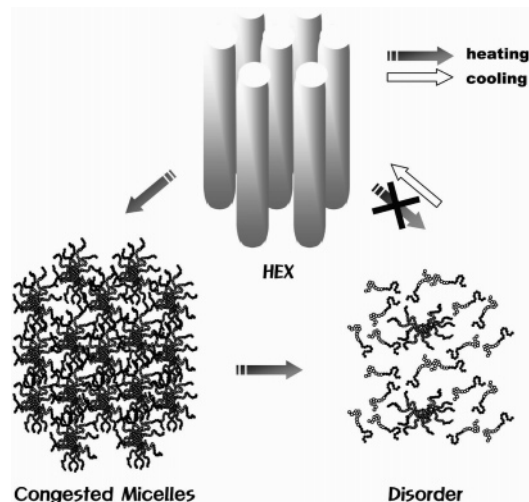


Figure 8. Schematic illustration of the transient state between the HEX phase and the disorder phase. During the heating scan, the disordered phase is reached through the transient state containing congested micelles from the HEX ordered phase while the disordered state quickly transforms into the HEX phase upon cooling.

formation of a liquidlike array of spherical micelles just above the ODT would be suppressed in melts, when the composition of the minor block exceeds about 22%. In our case, we have a concentrated solution in which the minor block, PI, would occupy approximately 20% of the solution volume if the PI domains were devoid of solvent. We do not know the precise distribution of solvent in these solutions, but we can conclude that as DBP is added to DEP the fraction of solvent in the PI core domains should increase or the effective composition of the PI domains would be increased. Thus, the disappearance of the transient congested micellar phase with decreasing solvent selectivity could be due to the disappearance of the disordered micellar phase itself. More studies with partially deuterated polymers would be necessary to address this issue any further.

On the basis of the results obtained so far, a schematic illustrating the pathways through the regions of HEX, solidlike spheres, and disordered micelles during heating and cooling scans is given in Figure 8. The HEX lattice undergoes the ODT via transient solidlike spheres upon heating while the disordered micelles prefer to pack directly into the hexagonal cylinders upon cooling. It is not likely that long wormlike micelles directly can disintegrate from the HEX phase, and instead, the HEX lattice prefers undulation into spherical micelles with a higher number density of hard spheres but lacks the long-range ordering due to intense fluctuation in block copolymer solution.

Conclusion

We have examined the solution behavior just above T_{ODT} by rheology and SAXS of a symmetric PS-*b*-PI diblock copolymer in PS-selective solvents, by varying the degree of solvent selectivity for PS: DEP > DEP/DBP (75:25 vol %) > DEP/DBP (50:50 vol %). The solutions undergo the two-step transitions, one between the HEX phase and a transient phase with a solidlike rheological response and the other to a disordered liquid of micelles. The solidlike behavior was observed in the log–log plots of G' and G'' against frequency ω . The temperature range of the solidlike response decreases with the decrease in solvent selectivity, and for the least selective system, i.e., DEP/DBP (50:50 vol %) solution, it is almost difficult to locate such a two-step transition region. The solidlike structures are transformed into disordered micelles upon an-

nealing at a constant temperature just above T_{ODT} , implying the transient characteristics. In addition, a key factor for the induction time for the dissolution of solidlike spheres is the solvent selectivity. The transient solidlike spheres of the DEP solution are quite stable for a few hours, whereas those of the DEP/DBP (75:25) solution are dissociated into disordered micelles after 1000 s of annealing, and dissolution occurs within a few seconds for the DEP/DBP (50:50) solution.

Acknowledgment. This work was supported by the NANO Systems Institute, National Core Research Center, from the Korea Science and Engineering Foundation, the Brain Korea 21 Program endorsed by the Ministry of Education of Korea, and the MRSEC program of the National Science Foundation under Award Number DMR-0212302. J.K.K. acknowledges the support of the National Creativity Research Initiative Program supported by the Korea Science and Engineering Foundation. We are also very grateful for the use of Pohang Light Source supported by the Ministry of Science and Technology of Korea.

References and Notes

- (1) Leibler, L. *Macromolecules* **1980**, *13*, 1602.
- (2) Helfand, E.; Wasserman, Z. R. *Developments in Block Copolymers*; Goodman, I., Ed.; Applied Science: New York, 1985; Chapter 4.
- (3) Fredrickson, G. H.; Helfand, E. *J. Chem. Phys.* **1987**, *87*, 697.
- (4) Mortensen, K.; Pedersen, J. S. *Macromolecules* **1993**, *26*, 805.
- (5) Bates, F. S.; Rosedale, J. H.; Fredrickson, G. H. *J. Chem. Phys.* **1990**, *92*, 6255.
- (6) Rosedale, J. H.; Bates, F. S. *Macromolecules* **1990**, *23*, 2329.
- (7) Rosedale, J. H.; Bates, F. S.; Almdal, K.; Mortensen, K.; Wignall, G. D. *Macromolecules* **1995**, *28*, 1429.
- (8) Almdal, K.; Bates, F. S.; Mortensen, K. *J. Chem. Phys.* **1992**, *96*, 9122.
- (9) Hashimoto, T.; Shibayama, M.; Kawai, H. *Macromolecules* **1983**, *16*, 361.
- (10) Almdal, K.; Mortensen, K.; Ryan, A. J.; Bates, F. S. *Macromolecules* **1996**, *29*, 5940.
- (11) Floudas, G.; Vazaiou, B.; Schipper, F.; Ulrich, R.; Wiesner, U.; Iatrou, H.; Hadjichristidis, N. *Macromolecules* **2001**, *34*, 2947.
- (12) Adams, J. L.; Quiram, D. J.; Graessley, W. W.; Register, R. A.; Marchand, G. R. *Macromolecules* **1996**, *29*, 2929.
- (13) Schwab, M.; Stühn, B. *Phys. Rev. Lett.* **1996**, *76*, 924.
- (14) Lodge, T. P.; Xu, X.; Ryu, C. Y.; Hamley, I. W.; Fairclough, J. P. A.; Ryan, A. J.; Pedersen, J. S. *Macromolecules* **1996**, *29*, 5955.
- (15) Holmqvist, P.; Pispas, S.; Hadjichristidis, N.; Fytas, G.; Sigel, R. *Macromolecules* **2003**, *36*, 830.
- (16) Maurer, W. W.; Bates, F. S.; Lodge, T. P.; Almdal, K.; Mortensen, K.; Fredrickson, G. H. *J. Chem. Phys.* **1998**, *108*, 2989.
- (17) Mori, K.; Okawara, A.; Hashimoto, T. *J. Chem. Phys.* **1996**, *104*, 7765.
- (18) Guenza, M.; Schweizer, K. S. *Macromolecules* **1997**, *30*, 4205.
- (19) Wang, J.; Wang Z.-G.; Yang, Y. *Macromolecules* **2005**, *38*, 1979.
- (20) Semenov, A. N. *Macromolecules* **1989**, *22*, 2849.
- (21) Semenov, A. N.; Anastasiadis, S. H.; Boudenne, N.; Fytas, G.; Xenidou, M.; Hadjichristidis, N. *Macromolecules* **1997**, *30*, 6280.
- (22) Matsen, M. W.; Schick, M. *Phys. Rev. Lett.* **1994**, *72*, 2660.
- (23) Dormidontova, E. E.; Lodge, T. P. *Macromolecules* **2001**, *34*, 9143.
- (24) Kudlay, A.; Stepanow, S. *J. Chem. Phys.* **2002**, *118*, 4272.
- (25) Sota, N.; Sakamoto, N.; Saijo, K.; Hashimoto, T. *Macromolecules* **2003**, *36*, 4534.
- (26) Sakamoto, N.; Hashimoto, T.; Han, C. D.; Kim, D.; Vaidya, N. Y. *Macromolecules* **1997**, *30*, 1621.
- (27) (a) Han, C. D.; Vaidya, N. Y.; Kim, D.; Shin, G.; Yamaguchi, D.; Hashimoto, T. *Macromolecules* **2000**, *33*, 3767. (b) Vaidya, N. Y.; Han, C. D.; Kim, D.; Sakamoto, N.; Hashimoto, T. *Macromolecules* **2001**, *34*, 222.
- (28) Choi, S.; Lee, K. M.; Han, C. D.; Sota, N.; Hashimoto, T. *Macromolecules* **2003**, *36*, 793.
- (29) Kim, J. K.; Lee, H. H.; Sakurai, S.; Aida, S.; Masamoto, J.; Nomura, S.; Kitagawa, Y.; Suda, Y. *Macromolecules* **1999**, *32*, 6707.
- (30) Wang, X.; Dormidontova, E. E.; Lodge, T. P. *Macromolecules* **2002**, *35*, 9687.
- (31) Adams, J. L.; Quiram, D. J.; Graessley, W. W.; Register, R. A.; Marchand, G. R. *Macromolecules* **1996**, *29*, 2929.
- (32) Hamley, I. W.; Fairclough, J. P. A.; Ryan, A. J.; Ryu, C. Y.; Lodge, T. P.; Gleeson, A. J.; Pedersen, J. S. *Macromolecules* **1998**, *31*, 1188.
- (33) Park, M. J.; Char, K.; Bang, J.; Lodge, T. *Macromolecules* **2005**, *38*, 2449.

- (34) Abuzaina, F. M.; Patel, A. J.; Mochrie, S.; Narayanan, S.; Sandy, A.; Garetz, B. A.; Balsara, N. P. *Macromolecules* **2005**, *38*, 7090.
- (35) Pedersen, J. S. *J. Chem. Phys.* **2001**, *114*, 2839.
- (36) Hanley, K. J.; Lodge, T. P.; Huang, C.-I. *Macromolecules* **2000**, *33*, 5918.
- (37) Lodge, T. P.; Hanley, K. J.; Pudil, B. *Macromolecules* **2002**, *35*, 4707.
- (38) Balsara, N. P.; Perahia, D.; Safinya, C. R.; Tirrell, M.; Lodge, T. P. *Macromolecules* **1992**, *25*, 3896.
- (39) Wang, H.; Newstein, M. C.; Chang, M. Y.; Balsara, N. P.; Garetz, B. A. *Macromolecules* **2000**, *33*, 3719.
- (40) Wang, C. Y.; Lodge, T. P. *Macromolecules* **2002**, *35*, 6997.
- (41) Park, M. J.; Char, K.; Bang, J.; Lodge, T. P. *Langmuir* **2005**, *21*, 1403.
- (42) Bang, J.; Lodge, T. P. *J. Phys. Chem. B* **2003**, *44*, 12071.
- (43) Elemans, P. H. M.; Janssen, J. M. H.; Meijer, H. E. H. *J. Rheol.* **1990**, *34* (8), 1311.